arXiv:1107.3005v1 [cond-mat.dis-nn] 15 Jul 2011

# Ferromagnetic-glassy transitions in three-dimensional Ising spin glasses

Giacomo Ceccarelli,[1] Andrea Pelissetto,[2] and Ettore Vicari[1]

[1] *Dip. Fisica dell'Università di Pisa and INFN, Largo Pontecorvo 2, I-56127 Pisa, Italy and*

[2] *Dip. Fisica dell'Università di Roma "La Sapienza" and INFN, P.le Moro 2, I-00185 Roma, Italy*

(Dated: July 13, 2011)

## Abstract

We investigate the ferromagnetic-glassy transitions which separate the low-temperature ferromagnetic and spin-glass phases in the temperature-disorder phase diagram of three-dimensional Ising spin-glass models. For this purpose, we consider the cubic-lattice $\pm J$ (Edwards-Anderson) Ising model with bond distribution $P(J) = p\delta(J-1) + (1-p)\delta(J+1)$, and present a numerical Monte Carlo study of the critical behavior along the line that marks the onset of ferromagnetism.

The finite-size scaling analysis of the Monte Carlo data shows that the ferromagnetic-glassy transition line is slightly reentrant. As a consequence, for an interval of the disorder parameter $p$, around $p \approx 0.77$, the system presents a low-temperature glassy phase, an intermediate ferromagnetic phase, and a high-temperature paramagnetic phase. Along the ferromagnetic-glassy transition line magnetic correlations show a universal critical behavior with critical exponents $\nu = 0.96(2)$ and $\eta = -0.39(2)$. The hyperscaling relation $\beta/\nu = (1+\eta)/2$ is satisfied at the transitions, so that $\beta/\nu = 0.305(10)$. This magnetic critical behavior represents a new universality class for ferromagnetic transitions in Ising-like disordered systems. Overlap correlations are apparently not critical and show a smooth behavior across the transition.

PACS numbers: 75.50.Lk,05.70.Fh,64.60.F-,05.10.Ln

## I. INTRODUCTION

Spin glass models are simplified, although still quite complex, models retaining the main features of physical systems which show glassy behavior in some region of their phase diagram. They may be considered as theoretical laboratories where the combined effects of disorder and frustration can be investigated. Their phase diagram and critical behavior can be used to interpret the experimental results for complex materials. Ising-like spin glasses, such as the $\pm J$ Ising model,[1] model disordered uniaxial magnetic materials characterized by random ferromagnetic and antiferromagnetic short-ranged interactions, such as $Fe_{1-x}Mn_xTiO_3$ and $Eu_{1-x}Ba_xMnO_3$; see, e.g., Refs. 2–4. The random nature of the short-ranged interactions is mimicked by nearest-neighbor random bonds.

Three-dimensional (3D) Ising spin glasses have been widely investigated. At low temperatures they present ferromagnetic and glassy phases, depending on the amount of frustration. The critical behaviors along the finite-temperature paramagnetic-ferromagnetic and paramagnetic-glassy (PG) transition lines have been accurately studied.[5–12] On the other hand, the low-temperature behavior, in particular the nature of the glassy phase and of the boundary between the ferromagnetic and glassy phases, is still debated.

In this paper we focus on the low-temperature transition line which separates the ferromagnetic phase, characterized by a nonzero magnetization, and the spin-glass (glassy) phase in which the magnetization vanishes while the overlap expectation value remains nonzero. We consider the 3D $\pm J$ Ising model, defined by the Hamiltonian[1]

$$H = -\sum_{\langle xy \rangle} J_{xy}\sigma_x\sigma_y, \tag{1}$$

where $\sigma_x = \pm 1$, the sum is over the nearest-neighbor sites of a cubic lattice, and the exchange interactions $J_{xy}$ are uncorrelated quenched random variables with probability distribution

$$P(J_{xy}) = p\delta(J_{xy} - 1) + (1 - p)\delta(J_{xy} + 1). \tag{2}$$

The usual bimodal Ising spin glass model, for which $[J_{xy}] = 0$ (brackets indicate the average over the disorder distribution), corresponds to $p = 1/2$. For $p \neq 1/2$ we have $[J_{xy}] = 2p-1 \neq 0$, and ferromagnetic (or antiferromagnetic) configurations are energetically favored.

The phase diagram of the cubic-lattice $\pm J$ Ising model is sketched in Fig. 1. We only consider $p \geq 1/2$ because of the symmetry $p \to 1 - p$. While the high-temperature phase is

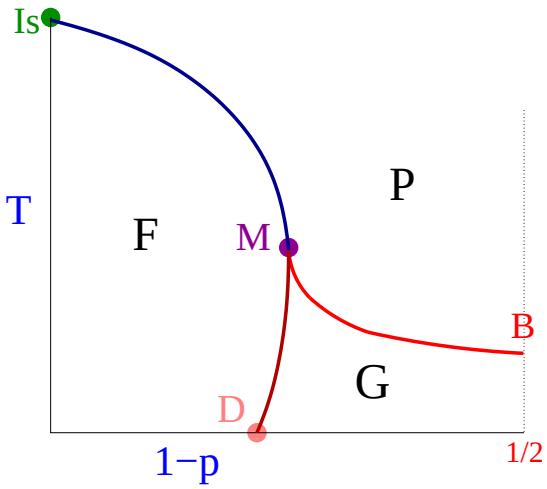



FIG. 1: (Color online) Temperature-disorder phase diagram of the 3D $\pm J$ Ising model. The phase diagram is symmetric under $p \to 1-p$ (but for small values of $p$ the system is antiferromagnetic).

always paramagnetic (P), at low temperatures there is a ferromagnetic (F) phase for small frustration, i.e., small values of $1-p$, and a glassy (G) phase with vanishing magnetization for sufficiently large frustration. In Fig. 1 we do not report any low-temperature mixed phase with simultaneous glassy and ferromagnetic behavior as found in mean-field models[13], for which, at present, there is no evidence.[14,15] The different phases are separated by transition lines belonging to different universality classes. They meet at a magnetic-glassy multicritical point M located along the so-called Nishimori line[16,17] $2/T = \ln[p/(1-p)]$, where the magnetic and the overlap two-point correlation functions are equal. Scaling arguments[18,19] show that the transition lines must be all parallel to the $T$ axis at the multicritical point M.

The paramagnetic-ferromagnetic (PF) transition line starts at the Ising transition of the pure system at $p = 1$, at[20] $T_{\rm Is} = 4.5115232(16)$, with a correlation-length exponent $\nu_{\rm Is} \approx 0.6301$ ($\nu = 0.63012(16)$ from Ref. 21 and $\nu = 0.63002(10)$ from Ref. 20). Along the PF line the magnetic critical behavior is universal,[5] and belongs to the randomly-dilute Ising universality class,[22,23] characterized by the correlation-length critical exponent $\nu_{\rm PF} = 0.683(2)$. It extends up to the multicritical point M, located at[19] $p_{\rm M} = 0.76820(4)$, $T_{\rm M} = 1.6692(3)$, whose multicritical behavior is characterized by two even relevant renormalization-group (RG) perturbations with RG dimensions $y_1 = 1.02(5)$ and $y_2 = 0.61(2)$. The paramagnetic-glassy (PG) transition line runs from M to the finite-temperature transition at $p = 1/2$, at[6] $T_{\rm B} = 1.11(1)$. The glassy critical behavior is universal along the PG line;[6] the overlap

correlation-length exponent is quite large,[6–11] $\nu_{\rm PG} = 2.45(15)$. Finally, (at least) another transition line is expected to separate the ferromagnetic and glassy phases. This is the ferromagnetic-glassy (FG) transition line that marks the onset of ferromagnetism and which runs from M down to the point D at $T = 0$. The nature and the general features of this transition line in Ising spin glasses are not known. Beside a few numerical works at $T = 0$,[14,15] this issue has never been investigated at finite temperature.

An interesting issue concerning the FG transition line is whether it is reentrant, which would imply the existence of a range of values of $p$ for which the glassy phase is separated from the paramagnetic phase by an intermediate ferromagnetic phase. As proved in Refs. 16, 17, ferromagnetism can only exist in the region $p > p_{\rm M}$, which implies that $p_{\rm D} \geq p_M$. We also mention that, using *entropic* arguments applied to frustration, the FG phase boundary was argued to run parallel to the $T$ axis,[17,24] i.e., $p_{\rm D} = p_{\rm M}$ for any $T < T_{\rm M}$, with the critical behavior controlled by a $T = 0$ *percolation* fixed point.[12] The FG transition was numerically investigated at $T = 0$ in Ref. 14, obtaining the estimate $p_{\rm D} = 0.778(5)$ for the critical disorder, which is slightly larger than $p_{\rm M} = 0.76820(4)$. Thus, it suggests a slightly reentrant FG transition line, although its apparent precision is not sufficient to exclude $p_{\rm D} = p_{\rm M}$.

In this paper we study the nature of the FG transition. In particular, we investigate whether the magnetic variables show a continuous and universal critical behavior from M to D, and whether hyperscaling is violated as it occurs in some systems whose critical behavior is controlled by a zero-temperature fixed point, like the 3D random-field Ising model.[25]

Note that we focus on the low-temperature ferromagnetic transition line, which marks the onset of ferromagnetism moving from the glassy phase with zero magnetization. There is also the possibility that a second low-temperature transition line exists for larger values of $p$. In this case there would be a mixed low-temperature phase, in which ferromagnetism and glassy order coexist. This occurs in mean-field models[13] such as the infinite-range Sherrington-Kirkpatrick model.[26] However, numerical $T = 0$ ground-state calculations in the 3D $\pm J$ Ising model on a cubic lattice[14] and in related models[15] do not seem to show evidence of a mixed phase and are consistent with a unique transition.

In this paper we present a Monte Carlo (MC) study of the critical behavior along the FG transition line. We perform simulations of finite systems defined on cubic lattices of size $L \leq 20$. A finite-size scaling (FSS) analysis of numerical data at $T = 0.5$ and $T = 1$ as

a function of $p$ shows that magnetic correlations undergo a continuous transition along the FG line. The critical behavior is universal, i.e., independent of $T$ along the line. For the magnetic critical exponents we obtain $\nu = 0.96(2)$ and $\eta = -0.39(2)$. Moreover, hyperscaling is verified. The FG transition line turns out to be slightly reentrant. Indeed, we find $p_c = 0.7729(2)$ at $T = 0.5$ and $p_c = 0.7705(2)$ at $T = 1$, which are definitely larger than the disorder parameter $p_M = 0.76820(4)$ at the multicritical point. Therefore, for a small interval of the disorder parameter, around $p \approx 0.77$, the phase diagram presents three different phases: a low-temperature glassy phase, an intermediate ferromagnetic phase, and a high-temperature paramagnetic phase.

Note that the critical behavior of the magnetic correlations along the FG transition line shows a new universality class of ferromagnetic transitions in Ising-like disordered systems, which differs from the randomly-dilute Ising universality class describing the critical behavior along the PF transition line, and from the random-field Ising universality class characterized by hyperscaling violation.

The general features of the phase diagram presented in Fig. 1 should also characterize the temperature-disorder phase diagram of other 3D Ising spin glass models with tunable disorder parameters. For example, one may consider models with Gaussian bond distributions, such as

$$P(J_{xy}) \sim \exp\left[-\frac{(J_{xy} - J_0)^2}{2\sigma}\right], \tag{3}$$

where the parameters $J_0$ and $\sigma$ control the amount of disorder (the pure ferromagnetic model corresponds to $J_0 > 0$ and $\sigma = 0$). This distribution is also characterized by the presence of a Nishimori line $T = \sigma/J_0$, where the magnetic and the overlap two-point correlation functions are equal. We also mention that an analogous temperature-disorder phase diagram, with three transition lines meeting at a multicritical point like Fig. 1, is also found in 3D XY gauge glass models.[27] A similar phase diagram is also expected for other continuous spin glasses, like XY and Heisenberg spin glasses with bond distributions (2) or (3).

The paper is organized as follows. In Sec. II we describe the MC simulations, and provide the definitions of the quantities we consider. Sec. III presents the FSS analysis of the MC data, reporting the main results of the paper. Finally, in Sec. IV we draw our conclusions. In the appendix we report some details of the FSS analyses.

## II. MONTE CARLO SIMULATIONS AND OBSERVABLES

In order to study the FG transition line, which connects points M and D in Fig. 1, we perform MC simulations of the $\pm J$ Ising model on cubic lattices of size $L$ with periodic boundary conditions. We use the Metropolis algorithm, the random-exchange method, and multispin coding. Implementation details can be found in Ref. 6. In the random-exchange simulations we consider $N_T$ systems at the same value of $p$ and at different temperatures in the range $T_{\rm max} \geq T_i \geq T_{\rm min}$, with $T_{\rm max} \gtrsim 2$ and $T_{\rm min} = 0.5$. The value $T_{\rm max}$ is chosen so that the thermalization at $T_{\rm max}$ is sufficiently fast—typically we take $T_{\rm max} \gtrsim T_M \approx 1.67$—while the intermediate values $T_i$ are chosen such that the acceptance probability for the temperature exchange is at least 10%. We require one of the $T_i$ to be along the Nishimori line.[16] The results for this temperature value can be compared with the known exact results and thus provide a check of the MC code and the thermalization. Finally, one of the temperatures always corresponds to $T = 1$. The parameter $N_T$ increases with $L$ and varies from $N_T = 5$ for $L = 4$ to $N_T = 19$ for $L = 20$. Thermalization is checked by verifying that disorder averages are stable when increasing the number of MC steps for each disorder realization. We average over a large number $N_s$ of disorder samples: $N_s \approx 2 \times 10^6$ samples for $L = 4, 6, 8$, $N_s \approx 3 \times 10^5$ for $L = 10$, $N_s \approx 10^5$ for $L = 12$, $N_s \approx 5 \times 10^4$ for $L = 16$, and $N_s \approx 5 \times 10^3$ for $L = 20$.

The simulations are quite costly, because of the very slow dynamics for low temperatures. This makes the computational effort increase with a large power of the lattice size. In our range of values of $L$, the number of iterations which must be discarded for thermalization apparently increases as $L^8$ for our largest lattices (with an increasing trend with increasing $L$). Hence, taking into account the volume factor, the CPU time for each disorder realization apparently increases as $L^{11}$ (but we should warn that its large-$L$ asymptotic behavior may be even worse). In total, simulations took approximately 40 years of CPU time on a single core of a recent standard commercial processor.

We consider the magnetization and the magnetic correlation function defined as

$$\begin{aligned} m &= \frac{1}{V}[\langle | \sum_x \sigma_x | \rangle], \\ G(x) &\equiv [\langle \sigma_0 \sigma_x \rangle], \end{aligned} \tag{4}$$

where the angular and the square brackets indicate the thermal and the quenched average

over disorder, respectively. We define the magnetic susceptibility and the second-moment correlation length, respectively as

$$\chi \equiv \sum_x G(x), \tag{5}$$
$$\xi^2 \equiv \frac{1}{4\sin^2(q_{\rm min}/2)} \frac{\widetilde{G}(0) - \widetilde{G}(q)}{\widetilde{G}(q)},$$

where $q = (q_{\rm min}, 0, 0)$, $q_{\rm min} \equiv 2\pi/L$, and $\widetilde{G}(q)$ is the Fourier transform of $G(x)$. Moreover, we consider the cumulants

$$U_4 \equiv \frac{[\mu_4]}{[\mu_2]^2}, \tag{6}$$
$$U_{22} \equiv \frac{[\mu_2^2] - [\mu_2]^2}{[\mu_2]^2},$$

where

$$\mu_k \equiv \langle (\sum_x \sigma_x)^k \rangle. \tag{7}$$

At the critical point $R_\xi \equiv \xi/L$, $U_4$, and $U_{22}$ (in the following we call them phenomenological couplings and denote them by $R$) are expected to approach universal values in the large-$L$ limit (within cubic $L^3$ systems with periodic boundary conditions). In the ferromagnetic phase we have $U_4 \to 1$, $U_{22} \to 0$, and $R_\xi \to \infty$, while in the glassy phase we expect $R_\xi \to 0$.

We also define analogous quantities using the overlap variables $q_x \equiv \sigma_x^{(1)}\sigma_x^{(2)}$, where $\sigma_x^{(1)}$ and $\sigma_x^{(2)}$ are two independent replicas corresponding to the same couplings $J_{xy}$. In particular, we consider $\xi_o$ and $U_4^o$ defined by replacing the magnetic variables with the overlap variables in Eqs. (5) and (6).

## III. FINITE-SIZE SCALING ANALYSIS

In this section we present a finite-size scaling (FSS) analysis of the MC data close to the FG transition line. We consider two values of the temperature, $T = 0.5$ and $T = 1$, below the temperature $T_M = 1.6692(3)$ of the multicritical point M, and perform a FSS analysis as a function of $p$.

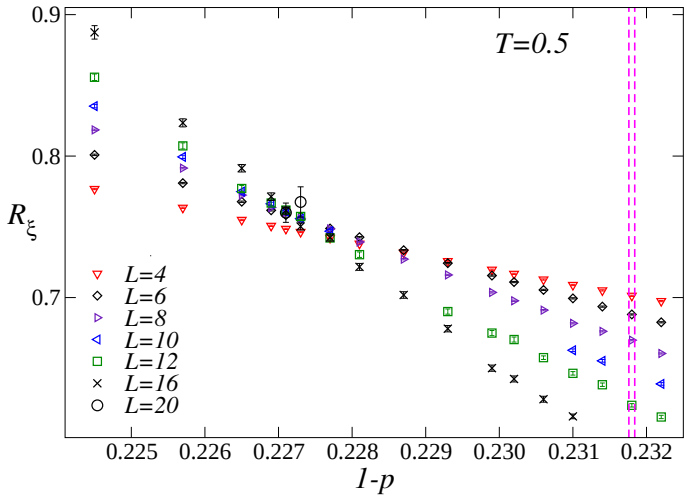



FIG. 2: (Color online) Estimates of $R_\xi$ at $T = 0.5$. The vertical lines show the location of the multicritical point M: $1 - p_M = 0.23180(4)$.

### A. Phenomenological couplings and universality

To begin with, we analyze the data at $T = 0.5$. In Fig. 2 we show the MC estimates of $R_\xi$ as a function of $1 - p$. Analogous plots are obtained for $U_4$ and $U_{22}$. The data for different lattice sizes clearly show crossing points, providing evidence for a continuous transition. They cluster at values of $p$ which are definitely larger than $p_M$, ruling out a vertical transition line from M to the $T = 0$ axis.

In the critical limit, the phenomenological couplings $R$ scale as

$$R = f_R[(p - p_c)L^{1/\nu}], \tag{8}$$

where we have neglected analytic and nonanalytic scaling corrections. Equivalently, one can test FSS by considering two different couplings $R_1$ and $R_2$. In the FSS limit $R_1 = F_{12}(R_2)$, where the function $F_{12}(R_2)$ is universal, i.e., identical in any model that belongs to a given universality class. Clear evidence of FSS is provided in Fig. 3, where the phenomenological couplings $U_4$ and $U_{22}$ are reported versus $R_\xi \equiv \xi/L$. The data appear to rapidly approach a nontrivial limit with increasing the lattice size. Scaling corrections are only visible in the case of $U_{22}$, but they decrease with increasing $L$.

In order to determine the critical parameter $p_c$ and the exponent $\nu$, we fit $U_4$, $U_{22}$, and

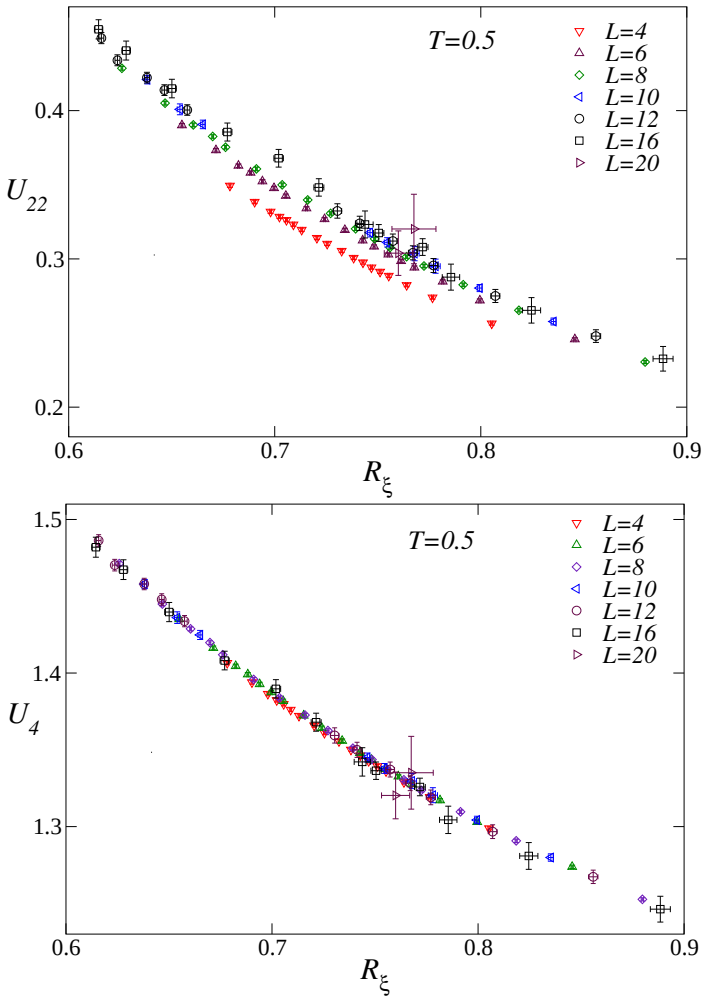



FIG. 3: (Color online) $U_4$ (bottom) and $U_{22}$ (top) vs $R_\xi$ at $T = 0.5$.

$R_\xi \equiv \xi/L$ to Eq. (8). Details are reported in App. A 1. We obtain

$$p_c(T = 0.5) = 0.7729(2), \qquad \nu = 0.96(2), \tag{9}$$

$$R_\xi^* = 0.764(6), \quad U_4^* = 1.331(5), \quad U_{22}^* = 0.305(2), \tag{10}$$

where $R^* = f_R(0)$ is the value of the phenomenological coupling $R$ at the critical point. Scaling corrections turn out to be small.

An analogous FSS analysis can be performed at $T = 1$, with the purpose of checking universality, i.e., of determining whether all transitions along the FG line belong to the same universality class. For this purpose, we use the fact that, given any pair of RG invariant quantities $R_1$ and $R_2$, the FSS function $R_1 = F_{12}(R_2)$ is universal. In Fig. 4 we plot $U_4$ and $U_{22}$ versus $R_\xi$ for both $T = 0.5$ and $T = 1$. The plot of $U_4$ provides good evidence of universality: all data fall onto a single curve with remarkable precision. The results for $U_{22}$

show instead significant scatter, but they are also consistent with universality if one takes into account scaling corrections: indeed, as $L$ increases the data for $T = 1$ approach the $T = 0.5$ results.

For a more quantitative check, we must explicitly take into account scaling corrections at $T = 1$, since they are significantly larger than those observed at $T = 0.5$. For instance, fits of the phenomenological couplings at $T = 1$ to Eq. (8) show a somewhat large $\chi^2$/DOF (DOF is the number of degrees of freedom of the fit). Moreover, the estimates show systematic trends as the lattices with smaller values of $L$ are discarded in the fit, see App. A 1 for details. To include scaling corrections, we fit the data to

$$R = f_R[(p - p_c)L^{1/\nu}] + L^{-\omega} g_R[(p - p_c)L^{1/\nu}]. \tag{11}$$

The smallest $\chi^2$/DOF is obtained for $0.8 \lesssim \omega \lesssim 0.9$. Correspondingly $\nu = 0.91(3)$, in substantial agreement with the estimate (9). Also the estimates of $R^*_\xi$, $U^*_4$, and $U^*_{22}$, see App. A 1, are in agreement with the estimates (10) at $T = 0.5$. Therefore, all results strongly support the universality of the critical behavior along the FG line. It is difficult to estimate reliably the exponent $\omega$ from the data. It we assume universality and fit the results at $T = 1$ fixing $\nu = 0.96(2)$, we obtain $\omega = 0.95(10)$. Note that the fits of the data at $T = 0.5$ give much larger values for $\omega$, i.e., $\omega \gtrsim 2$, see App. A 1. This is probably due to the fact that corrections with $\omega \approx 1$ have very small amplitudes at $T = 0.5$, so that we are simply measuring an effective exponent that mimicks the behavior of several correction terms.

The FSS fits also provide estimates of $p_c$ at $T = 1$. We obtain

$$p_c(T = 1) = 0.7705(2). \tag{12}$$

Note that $p_c(T = 1) > p_M \approx 0.7682$, conferming the reentrant nature of the FG transition line.

### B. Magnetic susceptibility

As discussed at length in Ref. 6, in the critical limit the magnetic susceptibility scales as

$$\chi(p, L) = u_h(p)^2 L^{2-\eta} f_\chi[(p - p_c)L^{1/\nu}], \tag{13}$$

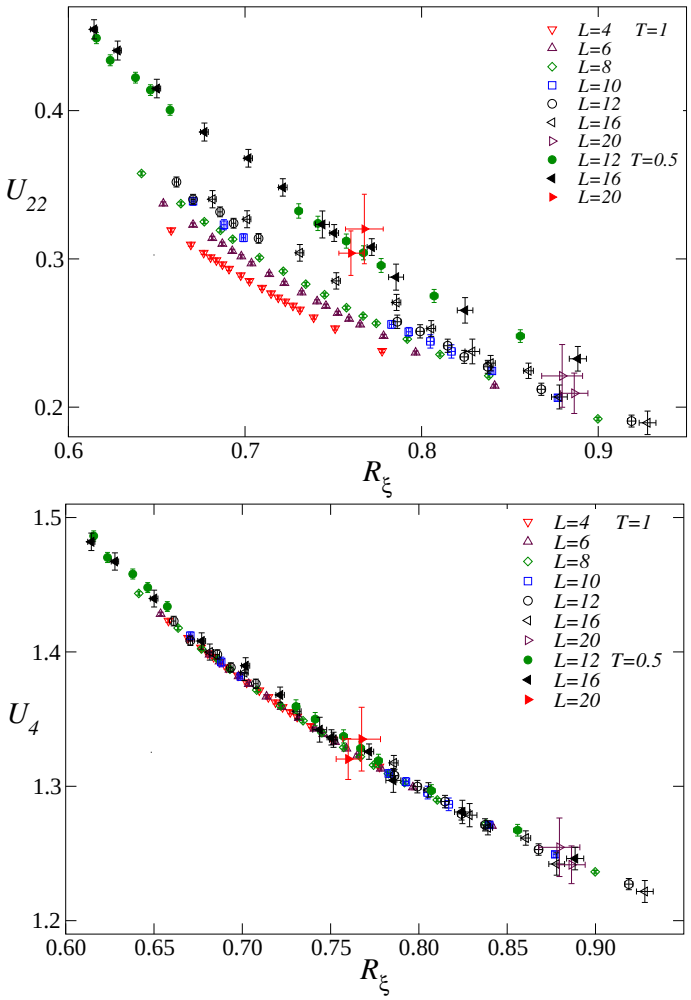



FIG. 4: (Color online) $U_4$ (bottom) and $U_{22}$ (top) vs $R_\xi$ at $T = 1$ and at $T = 0.5$ (only data with $L \geq 12$).

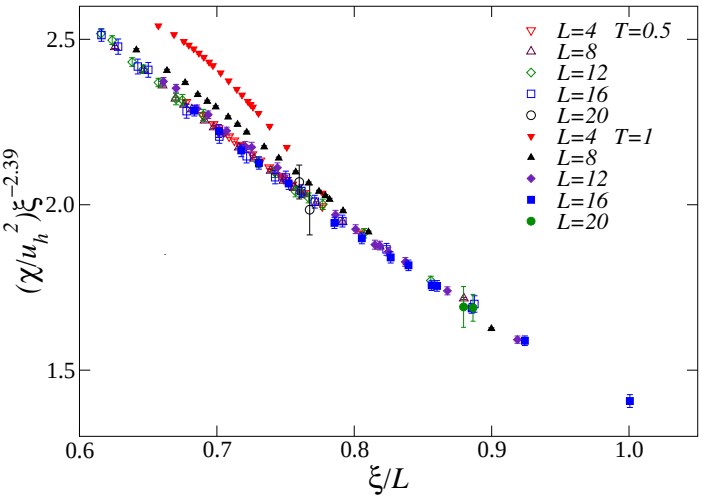



FIG. 5: (Color online) $\widetilde{\chi} \equiv \chi u_h^{-2} \xi^{-2.39}$ versus $\xi/L$ for $T = 1$ and $T = 0.5$.

where $u_h(p)$ is related to the magnetic scaling field and is an analytic function of $p$ (and also of the temperature). Fits of $\chi$ at $T = 1$ and $T = 0.5$ are good ($\chi^2$/DOF of order 1) if we include all data such that $L \geq 6$, provided that $u_h(p)$ is taken into account (see App. A 2 for details). We end up with the final estimate

$$\eta = -0.39(2). \tag{14}$$

Since $\xi/L$ is a function of $(p - p_c)L^{1/\nu}$ in the FSS limit, see Eq. (8), we can rewrite Eq. (13) as

$$\chi(p, L) = u_h(p)^2 \xi^{2-\eta} F_\chi(\xi/L). \tag{15}$$

The function $F_\chi(x)$ is universal apart from a multiplicative constant, which takes into account the freedom in the normalization of the function $u_h(p)$. In Fig. 5 we show the quantity $\widetilde{\chi} = \chi u_h^{-2} \xi^{-2.39}$ for $T = 1$ and $T = 0.5$. For each temperature the function $u_h(p)$ is determined by fitting the susceptibility data to Eq. (15), fixing $\eta = -0.39$. Moreover, the scaling fields are normalized so that $\widetilde{\chi}(T = 1, L = 16) \approx \widetilde{\chi}(T = 0.5, L = 16)$ for $\xi/L \approx 0.8$. If we discard the data with $L = 4$ and 8 at $T = 0.5$, all points fall on top of each other, confirming universality.

### C. Evidence of hyperscaling

Since the FG transition line extends up to $T = 0$, hence the critical behavior may be controlled by a zero-temperature fixed point, hyperscaling might be violated, as it happens in the 3D random-field Ising model.[25] In order to check whether hyperscaling holds along the FG line, we consider the magnetization, which is expected to behave as $m \sim L^{-\beta/\nu}$ at the critical point, and the magnetic susceptibility, which scales as $\chi \sim L^{2-\eta}$. If hyperscaling holds, $\beta$ and $\eta$ are related by

$$\frac{\beta}{\nu} = \frac{d - 2 + \eta}{2}, \tag{16}$$

(in the present case $d = 3$), which guarantees that $\chi/m^2$ scales as $L^d$. In order to verify whether Eq. (16) holds, we consider $H \equiv \chi/(m^2 L^3)$ and assume that it behaves as

$$H \equiv \frac{\chi}{m^2 L^3} \sim L^\zeta f_H[(p - p_c)L^{1/\nu}]. \tag{17}$$

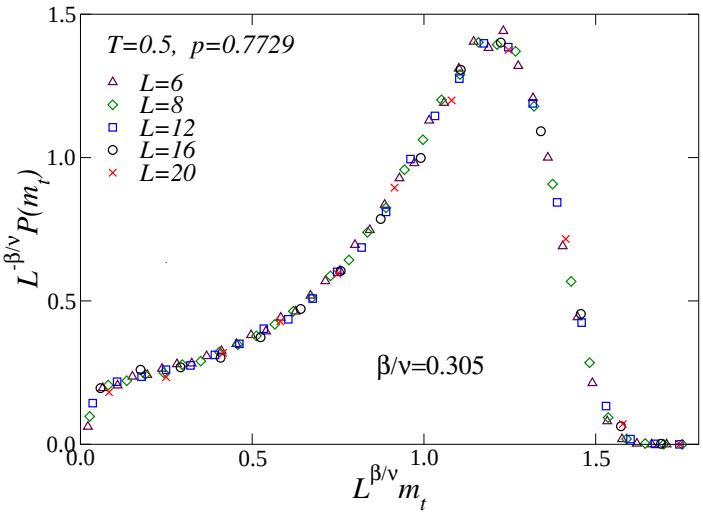



FIG. 6: (Color online) Scaling behavior of the distribution of the thermal averages of the magnetization, at $T = 0.5$ and $p = p_c = 0.7729$. We set $\beta/\nu = 0.305$.

If hyperscaling holds, $\zeta$ vanishes. A FSS analysis of the data at $T = 0.5$ and $T = 1$ gives the rather stringent bound (details in App. A 3)

$$|\zeta| < 0.01, \tag{18}$$

which allows us to conclude, quite confidently, that hyperscaling holds. If this the case, using estimates (14) and (9) of $\eta$ and $\nu$, we obtain

$$\beta/\nu = (1+\eta)/2 = 0.305(10), \qquad \beta = 0.29(1). \tag{19}$$

As a further check, we consider the sample distribution $P(m_t)$ of the thermal averages of the magnetization

$$m_t \equiv \frac{1}{V}\langle|\sum_x \sigma_x|\rangle \tag{20}$$

at the critical point $p = p_c = 0.7729$, $T = 0.5$, which is expected to behave asymptotically as

$$P(m_t) \approx L^{\beta/\nu}\mathcal{P}(L^{\beta/\nu}m_t). \tag{21}$$

In Fig. 6 we plot $\mathcal{P}(L^{\beta/\nu}m_t)$ using $\beta/\nu = 0.305$. The data clearly show the expected scaling behavior. In conclusion, the numerical results do not show evidence of hyperscaling violations in the critical behavior of magnetic correlations.

Our data for $H(p, L)$ can also be used to provide further evidence of universality. Indeed, if we use the fact that $\xi/L$ is a function of $(p - p_c)L^{1/\nu}$, see Eq. (8), we can rewrite Eq. (17)

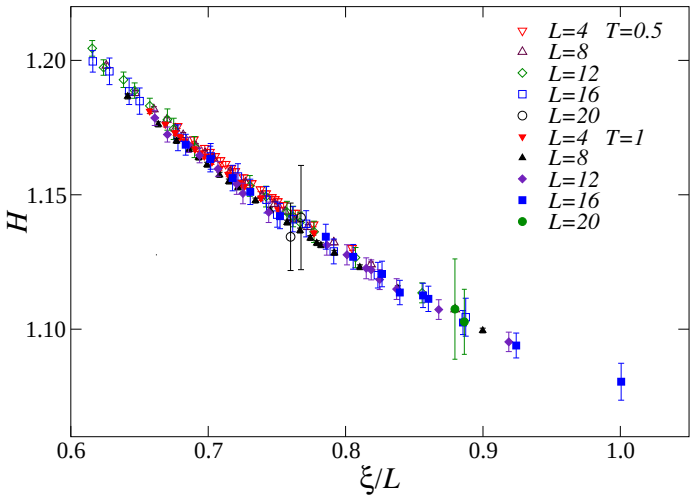



FIG. 7: (Color online) $H \equiv \chi/(m^2 L^3)$ versus $\xi/L$ for $T = 1$ and $T = 0.5$.

for $\zeta = 0$ as

$$H(p, L) = F_H(\xi/L) + O(L^{-\omega}), \tag{22}$$

where $F_H(x)$ should be the same at $T = 0.5$ and at $T = 1$ if all transitions along the FG transition line belong to the same universality class. The plot of the data, see Fig. 7, clearly confirms universality: all points fall onto a single curve.

### D. Overlap correlations

In our numerical study we also consider quantities involving the overlap variables, such as $\xi_o/L$ and $U_4^o$, defined at the end of Sec. II. In Fig. 8 we show MC data up to $L = 12$ (since their computation turned out to be significantly more demanding, we restricted the measurements for the lattices $L = 16$, 20 to the magnetic correlations). Unlike the magnetic quantities, the overlap data do not show crossings in the interval of $p$ we have investigated. Apparently $U_4^o$ decreases continuously, while $\xi_o/L$ increases as $L \to \infty$. This may reflect the fact that the FG transition line separates two *ordered* phases with respect to the overlap variables. Note that the differences between data at the same $p$ and $T$ and at different values of $L$ decrease as $1-p$ increases. Hence, if there is a line in the $(p, T)$ plane where the overlap variables show crossings, it must be such that $1 - p > 0.234$, i.e., it must lie in the region $p < p_M$, where no ferromagnetism is possible.

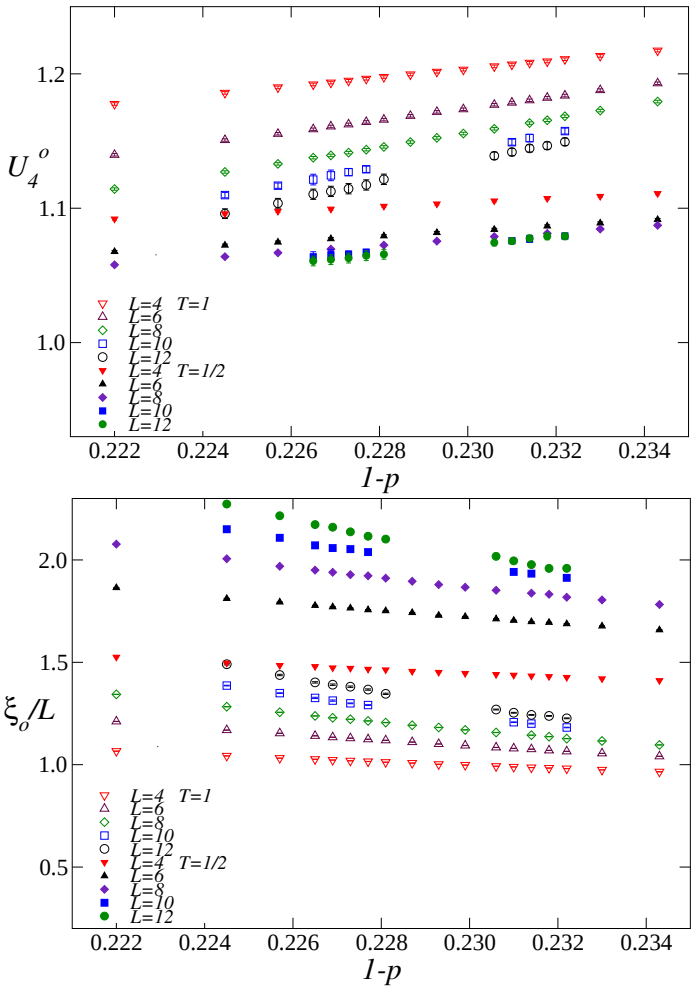



FIG. 8: (Color online) Estimates of $\xi_o/L$ (bottom) and $U_4^o$ (top), defined in terms of the overlap variables, at $T = 0.5$ and $T = 1$.

## IV. CONCLUSIONS

We investigate the critical behavior along the ferromagnetic-glassy transition line of the $T$-$p$ phase diagram of the cubic-lattice $\pm J$ (Edwards-Anderson) Ising model, cf. Eq. (1), which marks the low-temperature boundary between the ferromagnetic phase and the glassy phase where the magnetization vanishes, i.e., the transition line that runs from M down to the point D at $T = 0$ in Fig. 1.

We present a numerical study based on MC simulations of systems of size up to $L = 20$, obtaining MC estimates of several quantities at $T = 0.5$ and $T = 1$ (which are well below the temperature $T_M = 1.6692(3)$ of the multicritical point M) as a function of the disorder parameter $p$. The results of the FSS analyses are consistent with the two continuous magnetic

transitions belonging to the same universality class. The corresponding critical exponents are $\nu = 0.96(2)$ and $\eta = -0.39(2)$. Since the critical line extends up to $T = 0$, the critical behavior may be controlled by a zero-temperature fixed point. Correspondingly, it is possible to have hyperscaling violations, as it occurs in the 3D random-field Ising model. Our MC results show that the hyperscaling relation $\beta/\nu = (1 + \eta)/2$ is satisfied, so that $\beta/\nu = 0.305(10)$ and $\beta = 0.29(1)$. The FSS results provide a robust evidence of a universal magnetic critical behavior along the FG transition line. A reasonable hypothesis is that also the zero-temperature transition belongs to the same universality class. This is supported by the available numerical data at $T = 0$. The numerical study of Ref. 14 for the $\pm J$ Ising model at $T = 0$, using lattice sizes up to $L = 14$, provided evidence of a magnetic transition at $p_{\rm D} = 0.778(5)$, with critical exponents $\nu = 1.3(3)$ and $\beta = 0.2(1)$. Numerical analyses[15] for other Ising spin-glass models at $T = 0$ give consistent values of the critical exponents, $\nu = 0.9(2)$ and $\beta = 0.3(1)$ using data up to $L = 12$. These estimates are substantially consistent with our results along the FG transition line, supporting a universal critical behavior along the FG transition from the multicritical point M down to the $T = 0$ axis.

We also investigate the behavior of overlap correlations. They do not appear to be critical and show an apparently smooth behavior across the FG transition. Our numerical results do not show evidence of other transitions close to the transition line where ferromagnetism disappears. Thus, they do not hint at the existence of a mixed ferromagnetic-glassy phase, as found in mean-field models,[13] in agreement with earlier $T = 0$ numerical studies.[14,15]

The FG transition line is slightly reentrant. Indeed, we find that $p_c = 0.7729(2)$ at $T = 0.5$ and $p_c = 0.7705(2)$ at $T = 1$, which are definitely larger than $p_M = 0.76820(4)$, although they are quite close. This implies that there exists a small interval of the disorder parameter, around $p \approx 0.77$, showing three different phases when varying $T$: with increasing the temperature, the system goes from the low-temperature glassy phase with zero magnetization, to an intermediate ferromagnetic phase, and finally to the high-temperature paramagnetic phase. Correspondingly, it first undergoes a glassy-ferromagnetic transition with $\nu = 0.96(2)$ and then a ferromagnetic-paramagnetic transition with $\nu = 0.683(2)$. We mention that a slightly reentrant low-temperature transition line, where ferromagnetism disappears, also occurs in the phase diagram of the 2D $\pm J$ Ising model.[28,29]

The main features of the FG transition line are not expected to depend on the particular

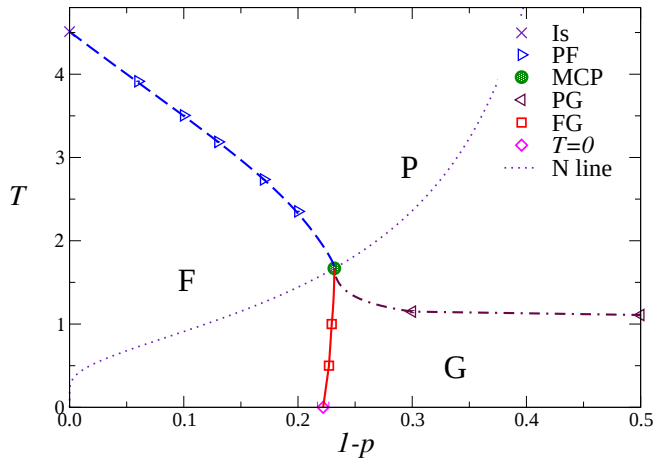



FIG. 9: (Color online) Numerical results for the phase boundaries of the cubic-lattice $\pm J$ Ising model (1) in the $T$-$p$ plane. The dashed lines are interpolations of the data[30].

discrete bond distribution of the $\pm J$ Ising model, cf. Eq. (2). They should also apply to more general distributions with tunable disorder parameters, such as the Gaussian distribution reported in Eq. (3), and also to experimental spin glass systems with tunable disorder.

We conclude showing Fig. 9 which reports all available numerical results for the phase boundaries of the cubic-lattice $\pm J$ Ising model (1) in the $T$-$p$ plane, taken from Ref. 5 for the PF transition line, from Ref. 19 for the multicritical point along the Nishimori (N) line $T = 2/\ln[p/(1-p)]$, from Ref. 6 for the data along the PG line, from this paper along the FG line, and from Ref. 14 for the $T = 0$ transition point. The dashed lines are interpolations of the data along the transition lines which satisfy the expected scaling behavior at the multicritical point where they meet, controlled by the crossover exponent $\phi = 1.67(10)$, see Refs. 19,28 for details.[30]

**Acknowledgments**

The MC simulations were performed at the INFN Pisa GRID DATA center, using also the cluster CSN4.

TABLE I: Results of combined fits of $U_4$, $U_{22}$, and $R_\xi$ to Eq. (A1) without scaling corrections. $\chi^2$ is the sum of the residuals in the fit and DOF is the number of degrees of freedom. Each column corresponds to results in which only data satisfying $L \geq L_{\rm min}$ are included. $R^* \equiv f_R(0)$ is the value of the phenomenological coupling at the critical point.

| | | | | |
|---|---|---|---|---|
| | | $T = 0.5$ | | |
| $L_{\rm min}$ | 4 | 6 | 8 | 10 |
| $\chi^2$/DOF | 5594/289 | 567/229 | 203/169 | 79/109 |
| $\nu$ | 0.971(4) | 0.964(5) | 0.954(8) | 1.00(2) |
| $p_c$ | 0.77230(1) | 0.77275(2) | 0.77284(3) | 0.77281(5) |
| $R_\xi^*$ | 0.7453(2) | 0.7564(3) | 0.7592(6) | 0.759(2) |
| $U_4^*$ | 1.3450(2) | 1.3364(4) | 1.3343(6) | 1.334(2) |
| $U_{22}^*$ | 0.3046(2) | 0.3045(3) | 0.3057(6) | 0.310(2) |
| | | $T = 1$ | | |
| $L_{\rm min}$ | 4 | 6 | 8 | 10 |
| $\chi^2$/DOF | 10593/289 | 1842/229 | 365/169 | 98/109 |
| $\nu$ | 1.054(5) | 0.995(5) | 0.963(8) | 0.982(20) |
| $p_c$ | 0.76819(2) | 0.76920(2) | 0.76975(3) | 0.76994(5) |
| $R_\xi^*$ | 0.6826(2) | 0.7019(3) | 0.7147(6) | 0.7220(17) |
| $U_4^*$ | 1.3973(3) | 1.3779(4) | 1.3662(6) | 1.3613(19) |
| $U_{22}^*$ | 0.3094(3) | 0.3020(4) | 0.2977(5) | 0.3013(17) |

## Appendix A: Analysis details

### 1. Phenomenological couplings

In order to determine the exponent $\nu$ and the critical parameter $p_c$, we analyze the phenomenological couplings $U_4$, $U_{22}$, and $R_\xi \equiv \xi/L$. In the critical limit each quantity $R$ behaves as

$$R(p, L) \approx f_R[u_p(p) L^{1/\nu}] + u_\omega(p) L^{-\omega} g_R[u_p(p) L^{1/\nu}], \tag{A1}$$

where the nonlinear scaling fields $u_p(p)$ and $u_\omega(p)$ are analytic functions of $p$. We have $u_p(p_c) = 0$ while, in general, we expect $u_\omega(p_c) \neq 0$. For both temperatures our data belong

to a small interval of values of $p$, so that we expect the approximations $u_p(p) \approx p - p_c$ and $u_\omega(p) \approx u_\omega(p_c) = a_\omega$ to work well. To check it, we also performed fits assuming $u_p(p) = p - p_c + k(p - p_c)^2$. We did not find any significant difference.

We first analyze the results at $T = 0.5$. We perform combined fits of the three quantities to Eq. (A1) without scaling corrections (we set $a_\omega = 0$). If the scaling functions $f_R$ are approximated by fourth-order polynomials, we obtain the results reported in Table I. We report estimates for different $L_{\rm min}$: in each fit we only include data satisfying $L \geq L_{\rm min}$. Corrections are quite small and indeed the results corresponding to $L_{\rm min} = 8$ and $L_{\rm min} = 10$ mostly agree within errors. We also perform fits that take into account scaling corrections. We fix $\omega$, approximate $g_R(x)$ by a second-order polynomial, and repeat the fit for several values of $\omega$ between 1 and 5. If we perform a combined fit of $U_4$ and $R_\xi$ (we include all results with $L \geq 4$), the smallest $\chi^2$/DOF (DOF is the number of degrees of freedom of the fit) is obtained for $3 \lesssim \omega \lesssim 4$ and one would estimate $\nu = 0.96(1)$ and $p_c = 0.7729(1)$. If instead we use $U_4$, $R_\xi$, and also $U_{22}$ we obtain $\omega \approx 2$, $\nu = 0.95(1)$, and $p_c = 0.7731(1)$. These results indicate that scaling corrections are quite small, and quite probably cannot be parametrized be a single correction term. Our best estimates of $\omega$ are simply effective exponents that parametrize the contributions of several different correction terms, which are all relevant for our small lattice sizes.

If we compare all results, we end up with the estimates $p_c = 0.7729(2)$ and $\nu = 0.96(2)$, reported in Eq. (9). For the phenomenological couplings at criticality, $R^* \equiv f_R(0)$, we obtain the estimates reported in Eq. (10), i.e., $R^*_\xi = 0.764(6)$, $U^*_4 = 1.331(5)$ and $U^*_{22} = 0.305(2)$. The final estimates and their errors take into account the results of the fits with and without scaling corrections.

The same analyses can be performed at $T = 1$. Combined fits to Eq. (A1) without scaling corrections give the results reported in Table I. It is quite clear that scaling corrections at $T = 1$ are larger then those at $T = 0.5$. The goodness of the fit is worse and the fit results show systematic trends. It is however reassuring that they apparently converge towards the estimates (9) and (10), in agreement with universality.

It is interesting to check whether scaling corrections can explain the differences which occur among the results for $T = 1$ reported in Table I and the results obtained at $T = 0.5$. Since the results for $U^*_{22}$ at $T = 1$ are nonmonotonic as a function of $L_{\rm min}$, at least two correction terms must be included to explain the observed trend of the data. Therefore,

TABLE II: Estimates of the exponent $\eta$ obtained by fits to Eq. (A3), where $\hat{f}_\chi$ is approximated by a fourth-order polynomial and $\hat{u}(p)$ by a second-order polynomial. In each fit we only include the data which satisfy $L \geq L_{\rm min}$. We fix $\nu = 0.96(2)$ and the value of $p_c$: $p_c = 0.7729(2)$ at $T = 0.5$ and $p_c = 0.7705(2)$ at $T = 1$.

| | $T = 0.5$ | | $T = 1$ | |
|---|---|---|---|---|
| $L_{\rm min}$ | $\chi^2$/DOF | $\eta$ | $\chi^2$/DOF | $\eta$ |
| 4 | 516/94 | −0.414(6) | 62/94 | −0.393(6) |
| 6 | 39/74 | −0.400(8) | 18/74 | −0.389(9) |
| 8 | 22/54 | −0.397(12) | 16/54 | −0.389(12) |
| 10 | 11/34 | −0.398(16) | 6/34 | −0.390(16) |

the fit of the $U_{22}$ data with a single scaling correction makes no sense. In any case, the estimate obtained for $L_{\rm min} = 10$ differs from the one reported in Eq. (10) by one combined error bar, and therefore is in agreement with universality. We then perform combined fits of $U_4$ and $\xi/L$ to Eq. (A1), approximating $g_R(x)$ by a second-order polynomial and fixing $\omega$ to several values between 0.5 and 1.5. The smallest $\chi^2$/DOF is obtained for $0.8 \lesssim \omega \lesssim 0.9$. Correspondingly, we obtain $p_c = 0.7705(1)$, $R^*_\xi = 0.765(10)$, and $U^*_4 = 1.32(1)$. The estimates of the phenomenological couplings at criticality are now in very good agreement with the estimates at $T = 0.5$. As for $\nu$ we obtain $\nu = 0.91(3)$, which is sligthly smaller than, but still consistent with the estimate at $T = 0.5$. If we fix $\nu = 0.96(2)$ as obtained at $T = 0.5$, we find $\omega = 0.95(10)$, $p_c = 0.7704(1)$, $R^*_\xi = 0.757(7)$, $U^*_4 = 1.326(6)$.

These fits provide an estimate of $p_c$ at $T = 1$. We quote the estimate $p_c = 0.7705(2)$ already reported in Eq. (12), which satisfies the inequality $p_c \gtrsim 0.7700$, which one would obtain from the results reported in Table I. It is unclear how reliable our estimates of $\omega$ are. In any case, they suggest a value close to 1.

### 2. Magnetic susceptibility

We analyze the magnetic susceptibility which should scale as

$$\chi(p, L) = u_h(p)^2 L^{2-\eta} f_\chi[u_p(p) L^{1/\nu}], \tag{A2}$$

TABLE III: Estimates of the exponent $\zeta$. In each fit we only include the data which satisfy $L \geq L_{\rm min}$. We fix $\nu = 0.96(2)$ and the value of $p_c$: $p_c = 0.7729(2)$ at $T = 0.5$ and $p_c = 0.7705(2)$ at $T = 1$.

| | $T = 0.5$ | | $T = 1$ | |
|---|---|---|---|---|
| $L_{\rm min}$ | $\chi^2$/DOF | $\zeta$ | $\chi^2$/DOF | $\zeta$ |
| 4 | 88/98 | $-0.007(2)$ | 161/98 | $-0.015(1)$ |
| 6 | 9/78 | $-0.003(2)$ | 15/78 | $-0.009(2)$ |
| 8 | 8/58 | $-0.002(3)$ | 3/58 | $-0.006(3)$ |
| 10 | 4/38 | $-0.005(5)$ | 2/58 | $-0.005(5)$ |

where $u_h(p)$ is related to the magnetic scaling field and is an analytic function of $p$; scaling corrections have been neglected. In order to determine $\eta$, we perform fits to

$$\ln \chi = (2 - \eta) \ln L + \hat{f}_\chi[(p - p_c)L^{1/\nu}] + \hat{u}(p), \tag{A3}$$

where $\hat{f}_\chi$ is approximated by a fourth-order polynomial and $u_h(p)$ is normalized so that $\hat{u}(p = p_c) = 0$. In this expression we have replaced $u_p(p)$ with $p - p_c$. Inclusion of the second-order term does not change the quality of the fit and the results. Instead, even if the interval in $p$ is small, the function $u_h(p)$ cannot be approximated by a constant, hence $\hat{u}(p)$ cannot be set to zero. Indeed, the fits in which $\hat{u}(p)$ is approximated by a second-order polynomial have a $\chi^2$/DOF which is significantly smaller than those in which we set $\hat{u}(p) = 0$. For instance, for $T = 0.5$ and $L_{\rm min} = 6$ (we fix $p_c$ and $\nu$, see caption of Table II), we have $\chi^2$/DOF = 265/76 and 39/74 for the fit with $\hat{u}(p) = 0$ and the fit with a second-order polynomial, respectively. The results of the fits in which we fix $\nu$ and $p_c$ are reported in Table II. The results are very stable with $L_{\rm min}$ and are completely consistent with universality. Note that, at variance with what is observed for the phenomenological couplings, corrections for $T = 1$ are apparently smaller than for $T = 0.5$. This may indicate the presence of several corrections which cancel out for our values of $L$. A conservative final estimate is $\eta = -0.39(2)$, already reported in Eq. (14).

### 3. Hyperscaling

In order to study hyperscaling we consider the ratio

$$H \equiv \frac{\chi}{m^2 L^3}. \tag{A4}$$

If hyperscaling holds, it should behave as

$$H(p, L) = f_h[u_p(p) L^{1/\nu}] \approx f_H[(p - p_c) L^{1/\nu}], \tag{A5}$$

where we have neglected scaling corrections. In order to allow for a possible hyperscaling violation we introduce a new exponent $\zeta$ and assume that

$$H(p, L) = L^{\zeta} f_H[(p - p_c) L^{1/\nu}]. \tag{A6}$$

To determine $\zeta$ we perform fits to

$$\ln H(p, L) = \zeta \ln L + \hat{f}_H[(p - p_c) L^{1/\nu}], \tag{A7}$$

where $\hat{f}_H(x)$ is approximated by a second-order polynomial. Fit results are reported in Table III. Here we fix $\nu$ and $p_c$ to the values determined above. The quality of the fits is very good and scaling corrections are apparently small for both values of the temperature. The exponent $\zeta$ is clearly compatible with zero, proving that hyperscaling is satisfied. More precisely, we obtain the bound $|\zeta| < 0.01$, already reported in Eq. (18).

---


[1] S. F. Edwards and P. W. Anderson, J. Phys. F **5**, 965 (1975).

[2] A. Ito, H. Aruga, E. Torikai, M. Kikuchi, Y. Syono, H. Takei, Phys. Rev. Lett. **57**, 483 (1986).

[3] K. Gunnarsson, P. Svedlindh, P. Nordblad, L. Lundgren, H. Aruga, and A. Ito, Phys. Rev. B **43**, 8199 (1991).

[4] S. Nair and A. K. Nigam, Phys. Rev. B **75**, 214415 (2007).

[5] M. Hasenbusch, F. Parisen Toldin, A. Pelissetto, and E. Vicari, Phys. Rev. B **76**, 094402 (2007).

[6] M. Hasenbusch, A. Pelissetto, and E. Vicari, Phys. Rev. B **78**, 214205 (2008); J. Stat. Mech.: Theory Exp. L02001 (2008).

[7] H. G. Katzgraber, M. Körner, and A. P. Young, Phys. Rev. B **73**, 224432 (2006).

[8] T. Jörg, Phys. Rev. B **73**, 224431 (2006).

[9] I. A. Campbell, K. Hukushima, and H. Takayama, Phys. Rev. Lett. **97**, 117202 (2006).

[10] H. G. Ballesteros, A. Cruz, L. A. Fernández, V. Martín-Mayor, J. Pech, J. J. Ruiz-Lorenzo, A. Tarancón, P. Téllez, C. L. Ullod, and C. Ungil, Phys. Rev. B **62**, 14237 (2000).

[11] M. Palassini and S. Caracciolo, Phys. Rev. Lett. **82**, 5128 (1999).

[12] N. Kawashima and H. Rieger, in *Frustrated Spin Systems*, edited by H.T. Diep (World Scientific, Singapore, 2004); cond-mat/0312432.

[13] G. Toulouse, J. Physique Lettres **41**, 447 (1980).

[14] A. K. Hartmann, Phys. Rev. B **59**, 3617 (1999).

[15] F. Krzakala and O. C. Martin, Phys. Rev. Lett. **89**, 267202 (2002).

[16] H. Nishimori, Prog. Theor. Phys. **66**, 1169 (1981).

[17] H. Nishimori, *Statistical Physics of Spin Glasses and Information Processing: An Introduction*, Oxford University Press, Oxford, 2001.

[18] A. Georges, D. Hansel, P. Le Doussal, and J. Bouchaud, J. Phys. (Paris) **46**, 1827 (1985); P. Le Doussal and A. B. Harris, Phys. Rev. Lett. **61**, 625 (1988).

[19] M. Hasenbusch, F. Parisen Toldin, A. Pelissetto, and E. Vicari, Phys. Rev. B **76**, 184202 (2007).

[20] M. Hasenbusch, Phys. Rev. B **82**, 174433 (2010).

[21] M. Campostrini, A. Pelissetto, P. Rossi, and E. Vicari, Phys. Rev. E **65**, 066127 (2002).

[22] A. Pelissetto and E. Vicari, Phys Rev. B **62**, 6393 (2000); D. V. Pakhnin and A. I. Sokolov, Phys. Rev. B **64**, 094407 (2001).

[23] M. Hasenbusch, F. Parisen Toldin, A. Pelissetto, and E. Vicari, J. Stat. Mech.: Theory Exp. (2007) P02016; P. Calabrese, V. Martìn-Mayor, A. Pelissetto, and E. Vicari, Phys. Rev. E **68**, 036136 (2003).

[24] H. Nishimori, J. Phys. Soc. Japan **55**, 3305 (1986);

[25] J. Villain, Phys. Rev. Lett. **52**, 1543 (1984); D. S. Fisher, Phys. Rev. Lett. **56**, 415 (1986).

[26] D. Sherrington and S. Kirkpatrick, Phys. Rev. Lett. **35**, 1792 (1975).

[27] V. Alba and E. Vicari, Phys. Rev. B **83**, 094203 (2011).

[28] F. Parisen Toldin, A. Pelissetto, E. Vicari, J. Stat. Phys. **135**, 1039 (2009); Phys. Rev. E **82**, 021106 (2010).

[29] M. Picco, A. Honecker, P. Pujol, J. Stat. Mech.: Theory Exp. (2006) P09006.

[30] An interpolation of the PF data with the correct scaling behavior at the multicritical point is provided by $p = 0.7682 + (0.59909 - \beta)^{\phi}(2.70487 - 9.03122\beta + 9.70235\beta^2)$, with $\beta \equiv 1/T$

and $\phi = 1.67$. In Fig. 9 the FG line with $T \geq 1$ is approximated by the line of equation[28] $p - p_M = a u_2(p,T)^\phi$, where $a \approx 0.03$ (which is fixed using our numerical estimate of $p_c$ at $T = 1$), $u_2(p,T) = \tanh\beta - 2p + 1$, and $p_M$ is the position of the multicritical point. For $T \leq 1$ we report the straight lines connecting the data at $T = 1$, 0.5 and $T = 0.5$, 0. Analogously, we proceed for the PG line, reporting the curve $p - p_M = c u_2(p,T)^\phi$ for $p \geq 0.7$ and a straight line for $0.5 \leq p \leq 0.7$.